19th Brazilian Congress of Thermal Sciences and Engineering
November 06th-10th, 2022, Bento Gonçalves - RS - Brazil

ENC-2022-0453
A NUMERICAL STUDY ON A H-DARRIEUS WIND TURBINE

Ramiro de Matos Bertolina
Rafael Castilho Faria Mendes
Universidade de Brasília, Department of Mechanical Engineer, Laboratory of Energy and Environment, 70910-900 Brasília ,DF, Brazil
ramirodematosbertolina@gmail.com
rafael.cfmendes@gmail.com

Antonio Brasil Junior
Universidade de Brasília, Department of Mechanical Engineer, Laboratory of Energy and Environment, 70910-900 Brasília ,DF, Brazil
Brasiljr@unb.br

Taygoara Felamingo de Oliveira
Universidade de Brasília, Department of Mechanical Engineer, Laboratory of Energy and Environment, 70910-900 Brasília ,DF, Brazil
Taygoara@unb.br

Abstract. *Although Horizontal Axis Wind Turbines (HAWTs) are more common in wind farms for electrical generation, Vertical Axis Wind turbines (VAWTs) have gained progressively more attention because they are suitable for installation inside urban centers or in highly variable wind direction conditions. In this work, we perform a numerical study of a three-bladed H-Darrieus wind turbine. The main goal of the work is to accurately reproduce the curve of power coefficient as a function of the tip speed ratio (non-dimensional power curve) for a given condition of non-disturbed flow. A periodic stall condition characterizes the flow around H-Darrieus turbine blades, and predicting the turbulence is challenging and critical to reliable power predictions. In this way, we perform a turbulence model assessment study considering κ-ε RNG, κ-ε Standard, and κ-ω SST. The values found for the performance coefficient are compared to experimental data available in the literature. We found that all three models can describe the abrupt boundary layer separation associated with the periodic stall, but the κ-ω SST presented results closest to the experimental reference, especially for the condition at maximal power generation. We also present results for the pattern of wall shear stress related to the stall.*

Keywords: *VAWT, Turbulence Model, CFD*

1. INTRODUCTION

In recent years, wind energy and other renewable energy sources have attracted the scientific community's attention (Scungio et al., 2016). The rising price of fossil fuels is driving energy diversification in developed countries while raising awareness of the rising level of greenhouse gases and global warming associated with exploiting non-traditional energy reserves (Bhuyan & Biswas, 2014). In this context, interest in the development of wind energy technology has grown significantly, as its energy production capacity is not influenced by political and economic instability (Scungio et al., 2016), (Bhuyan & Biswas, 2014).

Compared to Horizontal Axis Wind Turbines (HAWT), Vertical Axis Wind Turbines (VAWT) exhibit numerous advantageous characteristics. They are omnidirectional, offer low installation/maintenance costs, produce low noise emissions and perform well in turbulent conditions where unstable and distorted winds are predominant, making them ideal for urban environments (Eriksson et al., 2008). The VAWTs are divided between drag (Savonius) and lift (Darrieus) rotors. The H-Darrieus rotor exhibits the advantages of self-starting, high efficiency under low wind speeds, and higher peak speed rates (TSRs) compared to Savonius (Siddiqui et al., 2021).

Increasing studies are done to improve efficiency and extend the fields of application of turbines to all suitable locations. To demonstrate a turbine's performance and flow characteristics, a series of numerical simulation techniques, such as Vortex, Blade Element Momentum (BEM), Multiple Stream Tube Model, and Computational Fluid Dynamics

(CFD) models, for example, is the most cited models. However, the CFD model has become the most common model for research related to wind energy, as it provides more accurate data on the flow characteristics around wind turbines, such as the physics behind the dynamic stall (Paraschivoiu, 2002) compared to the other numerical models (Ghasemian et al., 2017).

Predicting unstable and highly turbulent flows, such as wind turbine stall dynamics, requires accurate and efficient computational models. In many cases, Unsteady Reynolds-Averaged Navier-Stokes (URANS) is used. However, turbulence models are often unreliable in predicting complex flow phenomena such as flow separation (Ghasemian et al., 2017), so verification with an experimental study is crucial. For example, the study by (Srinivasan et al., 1995) evaluated several turbulence models for unstable flows of a two-dimensional oscillating airfoil. The accuracy of force prediction in the flow regime strongly depended on the applied turbulence model.

Already (Siddiqui et al., 2021) carried out a study to discover the performance of H-Darrieus type VAWT at various levels of turbulence intensity and heights about the ground. For this, he analyzed three variations of the -ε turbulence model to verify the most suitable for the numerical study. As a result, it can be seen that the standard κ-ε model predicts a torque below the experimental one, while the κ-ε RNG model and the κ-ε Realizable model present values close to the experimental one. Nevertheless, the κ-ε Realizable turbulence model was chosen for the study, as it shows a prediction closer to reality than the other models.

Furthermore, Orlandi et al. (2015), in their study, made a preliminary analysis to obtain the best turbulence model for their wind turbine. The models considered were the most referenced for cases with strong adverse pressure gradients: κ-ε RNG and κ-ω SST (Shear Stress Transport). The performance coefficient (C_p) at different TSR values was the basis of the model comparison. The -ε RNG model presented a lower, as it presents overproduction in wall shear stresses, which led to a lower average torque value, so the κ -ω SST model was chosen to demonstrate the potential of a 3D RANS approach, unstable, to observe the effects of distorted winds on the power coefficient in an H-Darrieus turbine. Castelli et al. (2010) tested the -ε Realizable and κ-ω SST models, and it was possible to conclude that the κ-ε Realizable model is more suitable for 2D models, while the κ-ω SST is more suitable for 3D.

In this article, 3D URANS numerical simulations are proposed as a methodology since the 3D model can demonstrate the complex characteristics of the three-dimensional flow, such as dynamic stall (Orlandi et al., 2015). Therefore, to identify between the turbulence models κ-ε Standard, κ-ε RNG, and κ-ω SST, which can predict the torque closest to the experimental values found by Howell et al. (2010). The present study aims to reproduce a torque curve for the models mentioned above, understand how the torque and values are affected by each one, and compare with the literature results. According to the results, the κ-ω SST turbulence model obtained the value of the performance coefficient closest to the one found by Howell et al. (2010). In addition, it could better predict the problem's three-dimensional characteristics.

2. WIND TURBINE MODEL

2.1 VAWT modeling

Figure 1 shows the CAD model of the fixed pitch VAWT turbine. The H-rotor turbine is composed of 3 blades built with the airfoil profile, NACA 0022. The diameter (D) of the turbine is equal to 0.6 m, the blade chord length is 0.1 m, and the power rating of 11.79 W. The wind velocity is 4.31 m/s, and the tip speed ratio of 1.87.

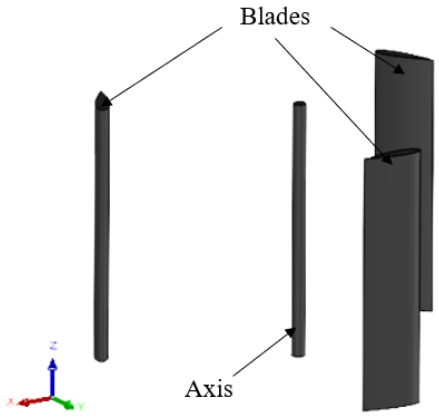

Figure 1. CAD model corresponding to turbine geometry. The turbine diameter is 0.6 m, and the blades have a height of 0.4 m. The wind speed is set to 4.31 m/s, and a tip speed ratio of 1.87.

Table 1. Turbine geometrical data.

Parameters	Values
Diameter (m)	0.6
Chord length (m)	0.1
Blade length (m)	0.4
Number of blades (-)	3
Inlet velocity (m/s)	4.31
Blade profile	NACA 0022

Figures 2 and 3 show the geometric model of the turbine placed inside a cylindrical domain to allow the rotation of the turbine during the transient simulation. The cylindrical domain was placed in another static domain with a length of 18R and a width of 8R, with R being the value of the radius of the turbine. The center of the coordinate system is located at the top of the turbine's central axis, with x being the streamwise and y being the cross-stream.

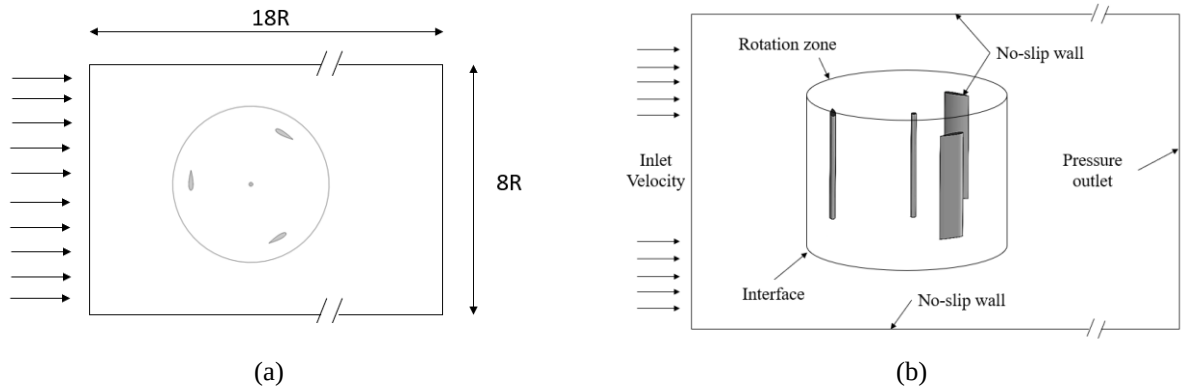

Figure 2. (a) Top view schematic of the computational model. (b) Wind turbine, flow domain, and boundary condition. The rotation zone is discretized using a sliding mesh.

2.2 Mesh generation and optimization

To obtain high-quality special discretization, the two domains had their meshes generated separately but consistently in the interface zone. In addition, the Sliding Mesh Rotating technique was applied in the interface zone, which allows modeling rotational effects in the rotational domain (rotor).

The mesh around the airfoils was created using the inflation tool, which models the region near the wall, to have a better description of the boundary layer, with 15 levels in the boundary layer of the airfoils, with the first layer having a height of 5.6×10^{-5} m so that y^+ = 1.45 and with a growth rate of 1.1. The rotational domain contains a mesh with 1,696,915 nodes, The mesh of the static domain contains 119,071 nodes. Within this mesh, a refinement was made in the wake region and the interface zone close to the rotational domain to maintain the spatial discretization refinement and accurately reproduce the interaction between the wake and the blades.

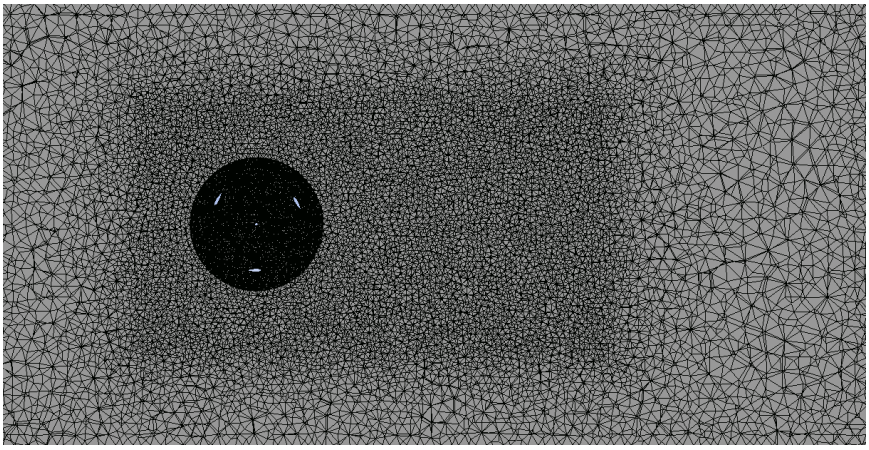

Figure 4. A numerical mesh is used to simulate the turbine. The existing refinement around the cylindrical domain was applied to ensure a good wake simulation. The total number of nodes in the mesh was 1,815,986.

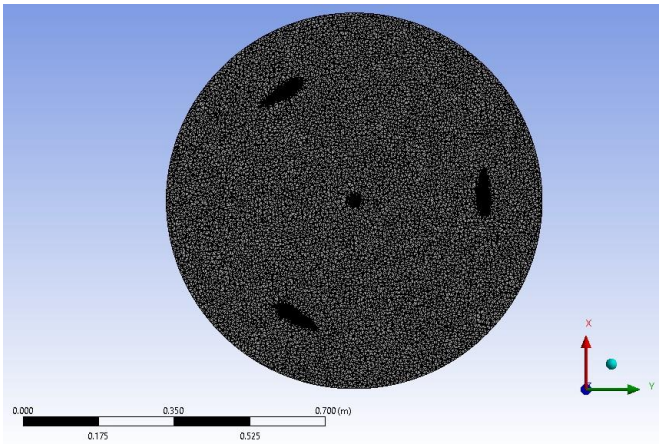

Figure 5. Horizontal cut view of the mesh inside the rotor.

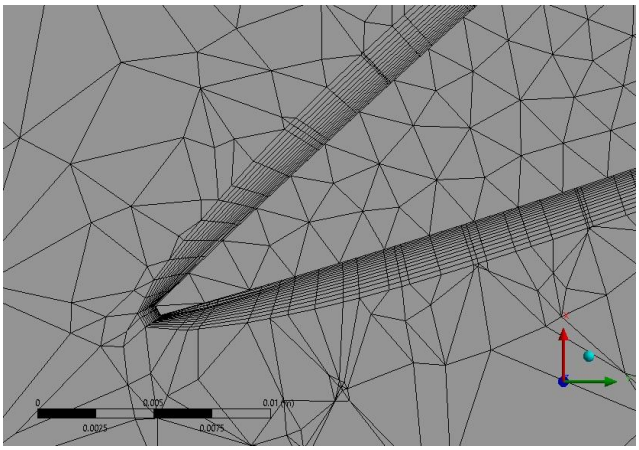

Figure 6. Inflation near the trailing edge of a blade.

2.3 Numerical method

Numerical simulations were performed in the finite volume CFX solver developed by Ansys. This study uses the implicit model equations (URANS) with the κ-ε Standard, κ-ε RNG, and κ-ω SST (Shear Stress Transport) turbulence models.

2.4 Boundary conditions and solver setup

The corresponding boundary conditions are imposed on the computational model. The top, bottom, front, and back boundary conditions are assigned slip conditions. The left side of the static domain has the input velocity condition with a velocity U_0=4.31 m/s. The right side has the output condition assigned a static pressure condition equal to 0. The geometric structure of the turbine is applied to the boundary condition without slipping. In the rotary domain, as illustrated in Figure 3, it performs circular movements with a tip-speed ratio of 1.87. The area where the two domains meet presents an interface condition. This study is based on the URANS implicit model, and the turbulence models used were the κ-ε Standard, κ-ε RNG, and κ-ω SST.

Transient type analysis with a timestep of 0.0021 seconds is fundamental for solving time-dependent CFD problems. A total of 7 VAWT revolutions were performed. However, the torque and C_p values will only be recorded from the two last laps.

3. RESULTS

3.1 Power curve

The performance of a given turbine is measured through the variation of torque and C_p as a function of the tip-speed ratio. The torque variation refers to the value produced by the turbine blades in one rotation. Figure 7 represents the evolution of the power coefficient as a function of the azimuthal position. The expression for C_p is defined as

$$C_p = \frac{T\omega}{\frac{1}{2}A_S U_0^3 \rho}, \tag{1}$$

where T is the torque value in $(N.m)$, ω is the rotation speed in (rad/s), A_S is the swept area in (m^2), U_0 is the wind speed in (m/s), and ρ is the density of the air in (kg/m^3). Figure 8 represents the evolution of the torque coefficient (C_t) as a function of the azimuthal position. The expression for Ct is defined as

$$C_t = \frac{T}{\frac{1}{2}A_S R U_0^2 \rho}. \tag{2}$$

The Tip-Speed Ratio (TSR) of a wind turbine is expressed as the ratio between the rotation speed of the rotor blade tip and the actual wind speed (U_0), that is, $TSR = \omega R/U_0$ where R is the value of the rotor radius. Therefore, VAWT's performance is heavily dependent on its TSR value.

Table 2. Comparison of the $\boldsymbol{\kappa}$-ε Standard, $\boldsymbol{\kappa}$-ε RNG and $\boldsymbol{\kappa}$-ω SST turbulence models with the values found for a TSR of 1.87. Values show average torque ($\boldsymbol{T_m}$) and average performance coefficient ($\boldsymbol{C_p}$).

Turbulence Model	T_m (Nm)	C_p
κ -ε Standard	0.0868	0.2115
κ -ε RNG	0.0876	0.2140
κ -ω SST	0.0731	0.1778

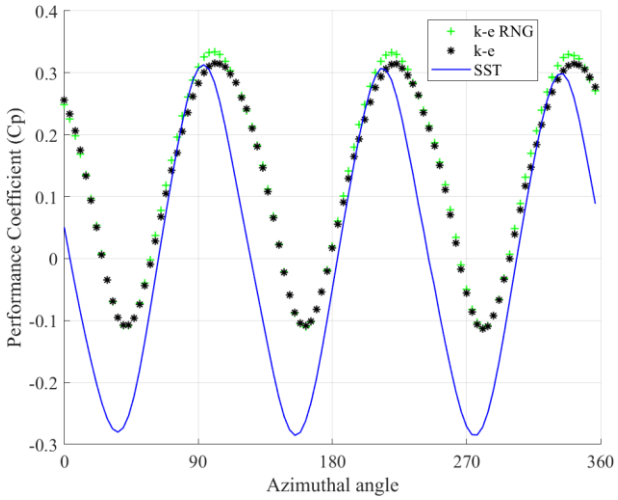

Figure 7. Performance coefficient for each turbulence model, calculated at TSR=1.87.

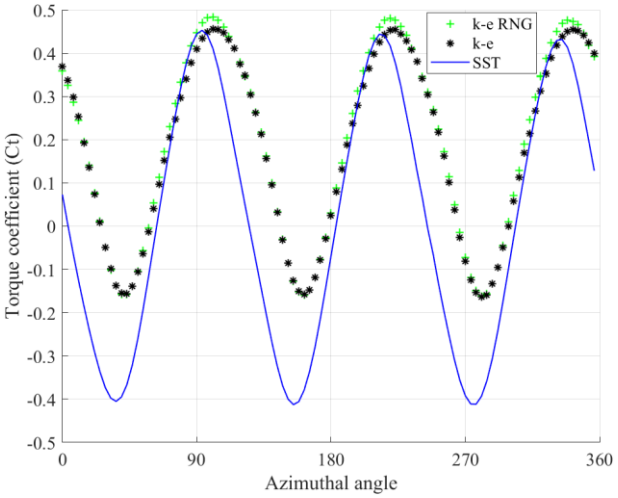

Figure 8. Torque coefficient for each turbulence model, calculated at TSR=1.87.

Table 3. Comparison of the κ-ε Standard, κ-ε RNG, and κ-ω SST turbulence models with the values found by Howell et al., 2010 for a TSR of 1.87. Values show performance coefficient (C_p).

	C_p
κ-ε Standard	0.2115
κ-ε RNG	0.2140
κ-ω SST	0.1778
Howell et al., 2010 3D model	0.1859
Howell et al., 2010 Experimental	0.1764 $\pm$20 %

3.2 Turbulence models assessment

Figure 9 shows the z-component of the vorticity of the flow predicted by κ-ε RNG (Figure 9(a)), κ-ε Standard (Figure 9(b)), and κ -ω SST (Figure 9(c)). Figure 10 shows the velocity field in the XY plane, produced by the turbine using the κ -ω SST turbulence model.

The three turbulence models show different contours for the z-component of the vorticity. However, the κ -ω SST model predicts a more abrupt displacement of the trailing vortex, found in Figure 9(a), indicated by the letter V, which occurs at position III in Figure 9(a). This is because the trailing vortex directly correlates with changes in the blade

pressure distribution, i.e., it directly influences the torque produced by the blade. Therefore, the ability of κ-ω SST to predict this phenomenon is associated with good accuracy in torque prediction.

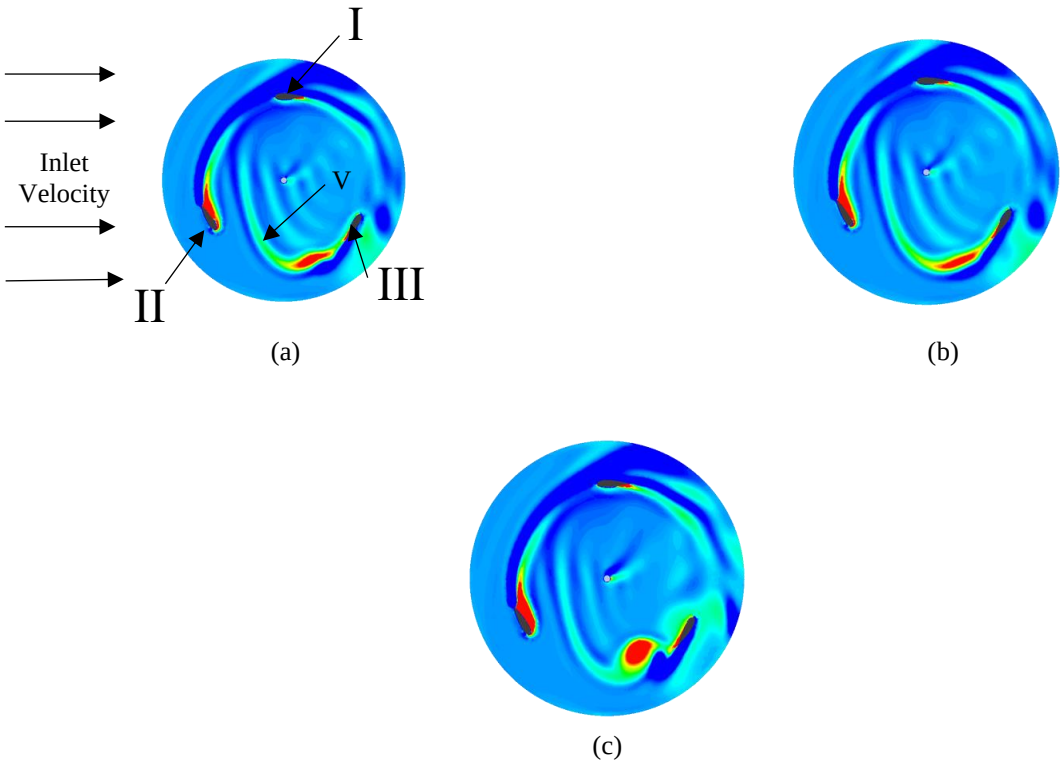

Figure 9. Vorticity1 in Z on the XY plane with a height of -0.2m, with different azimuthal positions (θ) for the turbulence models. For all letters, the blade I appear in the azimuthal position of 0°. Figure (a) used the κ-ε RNG turbulence model, (b) used the κ-ε Standard, and (c) used the κ -ω SST.

A horizontal plane is used in Figure 9 to visualize the tip of the rotor blades. This figure shows that the wake created by the trailing vortex is present in much of the area swept by the rotor blade. The region marked by the letter V in Figure 9 is the trail left by the previous rotor. The wake segment created by the blade flows following the flow direction. After some time, the segment will interact with the blade that created it. This will cause changes in the blade pressure distribution.

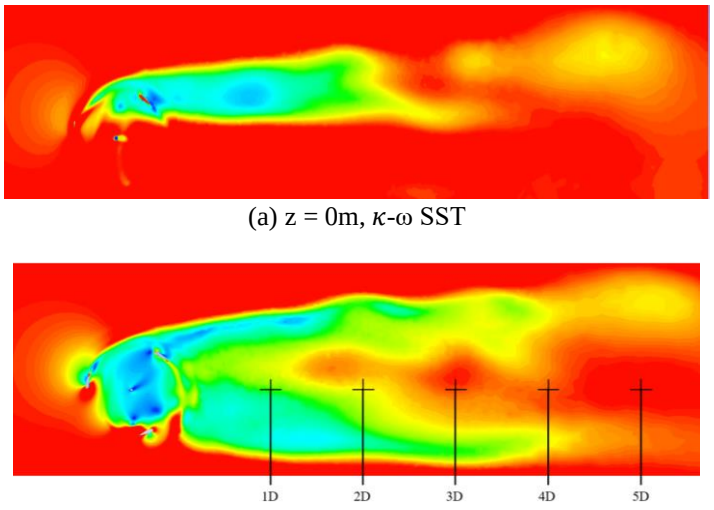

(a) z = 0m, *κ*-ω SST

(b) z = -0.2m, *κ* -ω SST

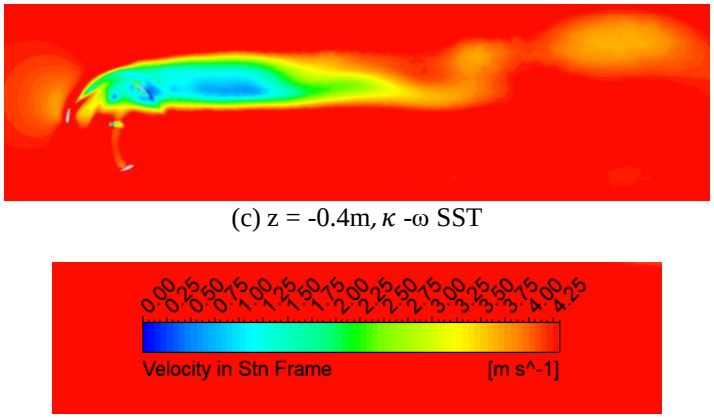

(c) z = -0.4m, κ -ω SST

Figure 10. Velocity field in the XY plane with three heights z=0m, z=-0.2m, and z=-4m for the $\boldsymbol{\kappa}$ -ω SST turbulence model. Figure 9 (b) had its wake divided into several segments equal to the rotor diameter.

During the revolution, the blade's passage decelerates the wind. That is, a loss of impulse is associated with the work extracted by the rotor. This wake follows the direction of the wind creating regions with low levels of thrust that is traversed by the back blade as it moves forward.

In figure 10, it can be noted that the presence of the turbine produces an adverse pressure gradient to the flow that reduces the velocity near the rotor. As a result, the wake produced by the VAWT is asymmetrical and deviates toward the region behind the blade in the movement of the wind. This asymmetry is created by the variation of aerodynamic forces about its azimuth position. The azimuthal variation can be reduced with increasing TSR and, in turn, will induce a more symmetrical wake (Khosravi et al., 2016). However, according to the velocity profiles with a distance of 5 times the diameter (D) of the turbine, the wake effects are minimal.

4. CONCLUSION

This study compares three turbulence models to identify the best model that best predicts turbine Cp for a specific TSR. A 3D URANS simulation was performed to find the results, analyzing the turbine Cp, torque, and three-dimensional flow effects.

With the results obtained, it was possible to conclude that the turbulence model κ-ε RNG and κ-ε Model presented the most distant results from the expected for Cp and torque. Furthermore, they could not predict the evolution of the trailing vortex separation.

The κ-ω SST model obtained the best results for the values of Cp and torque. It combines the accuracy and robustness of the κ-ω model in the region close to the wall with the free-flow insensitivity of the Standard κ-ε model in a transformed formulation away from the wall. The κ-ω SST could predict the evolution of the trailing vortex separation, making it the ideal model for predicting complex three-dimensional effects such as vorticity (Figure 9) and wake (Figure 10).

5. ACKNOWLEDGEMENTS

The Coordenação de aperfeiçoamento de Pessoal de Nível Superior (CAPES) for financial support.

6. REFERENCES

Bhuyan, S., & Biswas, A. (2014). Investigations on self-starting and performance characteristics of simple H and hybrid H-Savonius vertical axis wind rotors. *Energy Conversion and Management*, *87*, 859–867. https://doi.org/10.1016/j.enconman.2014.07.056

Castelli, M. R., Ardizzon, G., Battisti, L., Benini, E., & Pavesi, G. (2010). *IMECE2010-39548 MODELING STRATEGY AND NUMERICAL VALIDATION FOR A DARRIEUS VERTICAL AXIS MICRO-WIND TURBINE*. http://asme.org/terms

Eriksson, S., Bernhoff, H., & Leijon, M. (2008). Evaluation of different turbine concepts for wind power. *Renewable and Sustainable Energy Reviews*, *12*(5), 1419–1434. https://doi.org/10.1016/j.rser.2006.05.017

Ghasemian, M., Ashrafi, Z. N., & Sedaghat, A. (2017). A review on computational fluid dynamic simulation techniques for Darrieus vertical axis wind turbines. *Energy Conversion and Management*, *149*, 87–100. https://doi.org/10.1016/j.enconman.2017.07.016

Howell, R., Qin, N., Edwards, J., & Durrani, N. (2010). Wind tunnel and numerical study of a small vertical axis wind turbine. *Renewable Energy*, *35*(2), 412–422. https://doi.org/10.1016/j.renene.2009.07.025

Khosravi, M., Sarkar, P., & Hu, H. (2016, January 4). An Experimental Investigation on the Near Wake Characteristics of a Darrious Vertical-Axis Wind Turbine. *34th Wind Energy Symposium*. https://doi.org/10.2514/6.2016-1732

Orlandi, A., Collu, M., Zanforlin, S., & Shires, A. (2015). 3D URANS analysis of a vertical axis wind turbine in skewed flows. *Journal of Wind Engineering and Industrial Aerodynamics*, *147*, 77–84. https://doi.org/10.1016/j.jweia.2015.09.010

Paraschivoiu, I. (2002). Wind Turbine Design: With Emphasis on Darrieus Concept - Ion Paraschivoiu - Google Boeken. In *Presses Inter Polytechnique* (pp. 1–438).

Scungio, M., Arpino, F., Focanti, V., Profili, M., & Rotondi, M. (2016). Wind tunnel testing of scaled models of a newly developed Darrieus-style vertical axis wind turbine with auxiliary straight blades. *Energy Conversion and Management*, *130*, 60–70. https://doi.org/10.1016/j.enconman.2016.10.033

Siddiqui, M. S., Khalid, M. H., Zahoor, R., Butt, F. S., Saeed, M., & Badar, A. W. (2021). A numerical investigation to analyze effect of turbulence and ground clearance on the performance of a roof top vertical–axis wind turbine. *Renewable Energy*, *164*, 978–989. https://doi.org/10.1016/j.renene.2020.10.022

Srinivasan, G. R., Ekaterinaris, J. A., & McCroskey, W. J. (1995). Evaluation of turbulence models for unsteady flows of an oscillating airfoil. *Computers & Fluids*, *24*(7), 833–861. https://doi.org/10.1016/0045-7930(95)00016-6

7. RESPONSIBILITY NOTICE

The author(s) is (are) the only responsible for the printed material included in this paper.